EXPERIMENTAL MEASUREMENT AND NUMERICAL SIMULATION OF THE RUBBING FORCES BY TRANSIENT RESPONSE

Marcelo Braz de Aquino, braz@fem.unicamp.br
Robson Pederiva, Robson@fem.unicamp.br
Mechanical Design Department, Faculty of Mechanical Engineering, UNICAMP. Mendeleiev Street, Postal Code 13083-970, Campinas - SP- Brazil

Abstract. *This work is mainly focused on introducing a new experimental method to measure the rubbing force of the shaft against the mechanical seal in a multi-rotor system. The results gotten from the experimental test are compared to the simulated response modeled by Finite Element Method for describing such system. For analysis, the test rig is able to vary the stiffness of contact between the elements, the friction coefficient and the position along the shaft where the rubbing force occurs as well as the model does. Furthermore, it is easy to recognize the first touch of the shaft on the mechanical seal, and also, when this contact ends just by observing the quantities of force measured. The theoretical simulations shows that the contact occurs in frequencies near the natural ones where the vibration amplitudes are higher and more dangerous. One feature of this phenomenon happens when this contact starts, leading to unexpected dynamic behavior. So, in order to observe more clearly the mentioned instant and the period of time which the model pass through the critical speed, the transient response of the system was taken into account and simulated too.*

Keywords*: rubbing forces, rotor dynamic*

1. INTRODUCTION

The increase of efficiency is frequently linked to the decrease of radial clearance along the shaft in rotative machinery. Such systems are exposed to the occurrence of contact between its components when the clearances are reached by excessive vibrations. This phenomenon known by rubbing, with its effects, provokes an alteration on the rotor vibration patterns, when in fact it happens. These vibrations can be self-correcting (stable) or self-propagating (unstable), and in the worst case, the vibration can prohibit the machine operation (Sawicki *et al*, 2003).

Studied as an eventual phenomenon, is hoped that this contact does not happen on the system normal operation. But when it happens, it will be observed in the beginning as a partial or intermittent contact (the stationary-rotative system starts the contact and soon afterwards the same contact gets finish). During a complete period, the involved elements can be interacted once or fewer times. Alternated efforts are created in the shaft and the system can exhibit a complex vibration of investigate. Starting from this point, chaotic vibrations can be found in some circumstances. A gradual aggravation of the partial contact will take to the total or permanent rubbing (the contact is kept after its establishment), taking to appearing higher vibrations (Chu and Lu, 2005).

The type of fault studied here, will be always secondary due to a primary cause which disturbs the normal condition of the machine operation, see (Chu and Lu, 2001, Fatarella, 1999, Zhang *et al*, 2003). For instance, the unbalance, misalignment of thermal origin or due to the incorrect assembly, besides the fluid-dynamics forces that produces instability and self-excited vibrations.

A more detailed analysis of this phenomenon should involve several aspects as mentioned in the following (Piccoli, 1994): the beginning of the contact, if with impact or not; the subjects involved with the elasticity of the contact situation; the friction influence; the effects of thermal nature originated by the rubbing; and the contact dynamic behavior.

The studies about rub exhibit vibrations of chaotic and unexpected behavior clearly (Sawicki *et al*, 2003) and some names are often mentioned as reference of researches treating of the chaotic movement due to the rubbing, among them we can find Agnes Muszynska and Paul Goldman, see (Bently *et al*, 2002a, Bently *et al*, 2002b, Muszynska and Goldman, 1995).

Research groups has accomplished experimental tests and has confronted with numeric simulations in order to describe the influence of impacts in the behavior of flexible rotors interacting in flexible stators, see (Ehehalt and Markert, 2002, Wegener and Markert, 1998, Wegener *et al*, 1998). The authors concluded that the impacts happen during the non-stationary transitions between the states of the movement with and without contact and also if the flexible stator is misaligned in the rotor shaft direction. In recent studies (Ehehalt *et al*, 2005, Ehehalt *et al*, 2006a, Ehehalt *et al*, 2006b, Ehehalt *et al*, 2006c), with improvements in the mathematical model, they could reach patterns of movement that describes the contact between rotors and flexible stators as well as the description of backward whirl and synchronous forward whirl.

Also was commented by Bedoor (2000) that due to the fact that the rotor is never balanced perfectly, the contact will be more expected on the run-up period, when the rotor is passing through its critical speed. The author had investigated the torsional vibrations in addition to the lateral ones and its influences on dynamic behavior of the rubbing system.

Based on the researches accomplished in this area, it is not so difficult to judge if the system is suffering rubbing or not. For the partial contact, the wave form of rotor vibration will be truncated. And when the partial rubbing progresses for the permanent, the rotor vibration will show orbits of backward whirl which is the special fact that distinguishes this kind of fault between others. However, for the diagnosis purpose, its location continues being a difficult task, besides turning difficult the accomplishment of repetitive experiments, knowing that this malfunction might carry to a deterioration of the shaft and clearances enlargement by wear and deformations by thermal effects.

Bartha (2000) discusses about one possible solution for rub problem in turbomachinery, namely to avoid any contact between the rotor and stationary parts by designing large enough annular clearances, is not generally realizable since the clearances at the seal locations to a large degree determine the plant's efficiency and its competitiveness in the market. There will therefore always be a certain area of conflict between economical and safe operation.

Taking as example a gas turbine, where normally has big dimensions and small radial clearances between rotative and stationary elements, in the order to increase the clearances sufficiently trying to avoid that the shaft touch the mechanical seal, the machine's efficiency will be reduced due to the losses at this place where should guarantee certain difference of the gas pressure. Otherwise, if the radial clearance is sufficiently tight to guarantee that difference of pressure, the risk of contact occurrence will be increased.

The phenomenon of rubbing in rotative machines, more precisely the disk-stator rubs, has been largely studied for the last three decades in experimental and simulated analysis by the using of several tools to detect it and diagnose. The rubbing forces in this work are always introduced on the shaft instead of on the disk. The device which suffers the friction was developed to be able to vary stiffness and the friction coefficient between the elements with purpose of compare the experimental results with simulated ones.

In order to minimize the approaches that make the simulated system does not be realistic, the Finite Elements Method were implemented and introduced on the multi-rotor system as shown in further section. And also to detect the non-stationary behavior of the rubbing, the system has been studied through the transient responses that simulates the run-up of the machine, taking account the passages by the critical frequencies.

2. RUB FORCES

It is assumed that there is an initial static clearance δ between the shaft and seal. Comparing with one complete period of rotating, the time during rub is very short. Therefore, an elastic impact model was used, and also, the Coulomb type of frictional relationship is assumed in the analysis. When rub happens as shown in Fig. 1, the radial impact force F_N and the tangential rub force F_T can thus be expressed as (Aquino *et al*, 2006)

$$F_N(x,y) = \begin{cases} 0, & (for\ R < \delta) \\ (R-\delta)k_R, & (for\ R \geq \delta) \end{cases} \qquad (1)$$
$$F_T = f\,F_N$$

where f is the friction coefficient between shaft and seal, k_R the impact stiffness coefficient of the seal, R is the radial displacement of the shaft at seal position

$$R = \sqrt{x^2 + y^2} \qquad (2)$$

and these two forces can be written in x and y coordinates as

$$\begin{aligned} F_x(x,y) &= -F_N\cos\phi + F_T\sin\phi \\ F_y(x,y) &= -F_N\sin\phi - F_T\cos\phi \end{aligned} \qquad (3)$$

where ϕ is the angular displacement of the shaft. Finally, the rubbing forces can be rewritten as

$$\begin{Bmatrix} F_X \\ F_Y \end{Bmatrix} = H(R-\delta)\frac{(R-\delta)k_R}{R}\begin{bmatrix} 1 & -f \\ f & 1 \end{bmatrix}\begin{Bmatrix} x \\ y \end{Bmatrix} \qquad (4)$$

where H is a function described by

$$H(x) = \begin{cases} 0, & x \leq 0 \\ 1, & x > 0 \end{cases} \qquad (5)$$

The Eq. (4) indicates that when the displacement of the rotor R is smaller than the static clearance δ between the shaft and seal, the rubbing will not exist and its rub forces will be zero. Those forces will happen strictly when the displacement of the rotor R is larger than δ.

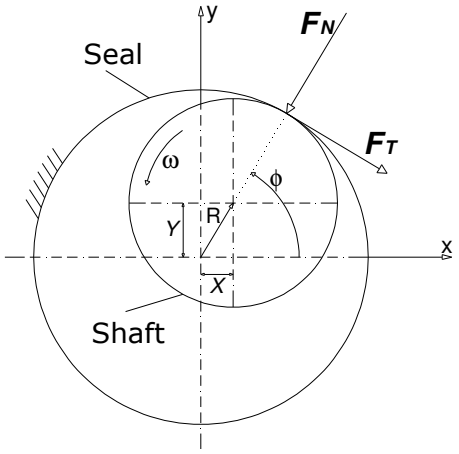

Figure 1: Scheme of rub forces.

3. MATHEMATICAL MODEL

According to Fig. 2, the model possesses 2 disks, both with mass equals to 4 kg described as elements number 6 and 11, and they can whirl with no restrictions at the position of nodes number 4 and 8, respectively. The system is supported on three identical bearings with damping equals to 42 Ns/m and stiffness 1.47×10^5 N/m, they are described as elements 1, 3 and 14 situated at the nodes 1, 2 and 10 respectively. The elements 2, 4, 5, 7, 8, 9, 10, 12 and 13 are all of them shaft elements. The shaft element number 2 has length equals to 60×10^{-3} m, and the others, 90×10^{-3} m. Each element possesses two degrees of freedom (x and y direction).

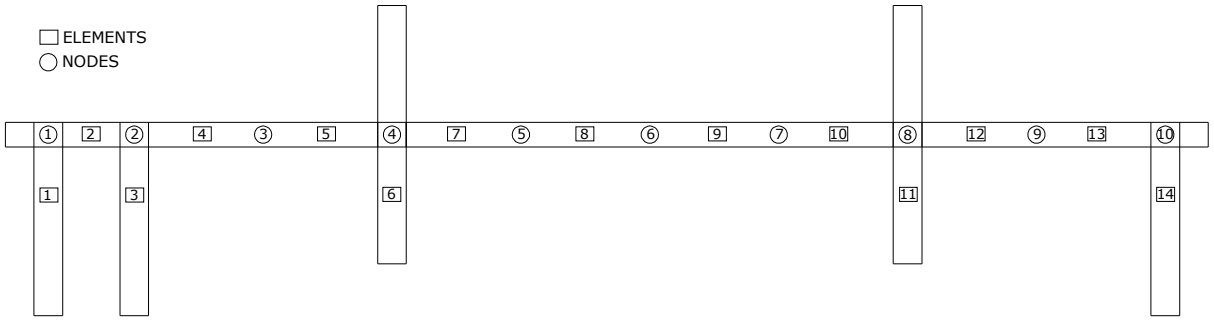

Figura 2. Finite element model discussed.

Starting from angular velocity ω_o, the rotor is accelerated in respect to the time t at a constant angular acceleration α and passes through the critical speed of the system. The rotative angle, velocity and acceleration can be expressed as

$$\phi = \frac{1}{2}\alpha t^2 + \omega_o t, \qquad \omega = \dot{\phi} = \alpha t + \omega_o, \qquad \ddot{\phi} = \alpha \tag{6}$$

The rubbing forces described in Eq. (4) were applied between the disks simulating the seal at the position of node number 6. Moreover, neglecting the torcional effects along the shaft, the unbalance forces of the disks were applied on the nodes number 4 and 8 according to following equations

$$\begin{aligned} F_{UX} &= mU(\ddot{\phi}\sin(\phi) + \dot{\phi}^2\cos(\phi)) \\ F_{UY} &= mU(\dot{\phi}^2\sin(\phi) - \ddot{\phi}\cos(\phi)) \end{aligned} \tag{7}$$

where m is the rotor mass, U is the unbalance, F_{UX} and F_{UY} are the x and y components of the unbalance force respectively.

The equation for transient motion applied here is given by

$$\left[[M_D]+[M_E]+[M_S]\right]\left\{\ddot{\xi}(t)\right\}+\left[[C_M]+\dot{\phi}[C_S]\right]\left\{\dot{\xi}(t)\right\}+\left[[K_M]+[K_S]+\ddot{\phi}[K_{ST}]\right]\left\{\xi(t)\right\}=\left\{F(t)\right\} \qquad (8)$$

where $\xi(t)$ is the vector of generalized coordinates. The matrices $[M_D]$, $[M_E]$ e $[M_S]$ are associated to mass of the disks, mass of shaft elements and rotational effect of the shaft, respectively. Furthermore, $[C_M]$ and $[C_S]$ are the matrices of bearings damping and gyroscopic of the shaft elements, respectively. And also, $[K_M]$, $[K_S]$ and $[K_{ST}]$ are the matrices of bearings stiffness, stiffness of shaft elements and stiffness of shaft elements in function of the rotation. An overview about the matrices is better demonstrated in (Lalanne and Ferraris, 1999).

4. TEST RIG

The experimental setup is shown in Fig. 3. A flexible coupling is connected between the induction motor and the shaft. The test rig has characteristics of simple structure, wide speed range, been stable and reliable. The rated current of the electric motor is 8.43 A and the output power is 2.2 kW. The rotating speed can be adjusted between 0 and 3600 rev/min. The rotating shaft has a diameter of 17 mm with total length of 840 mm.

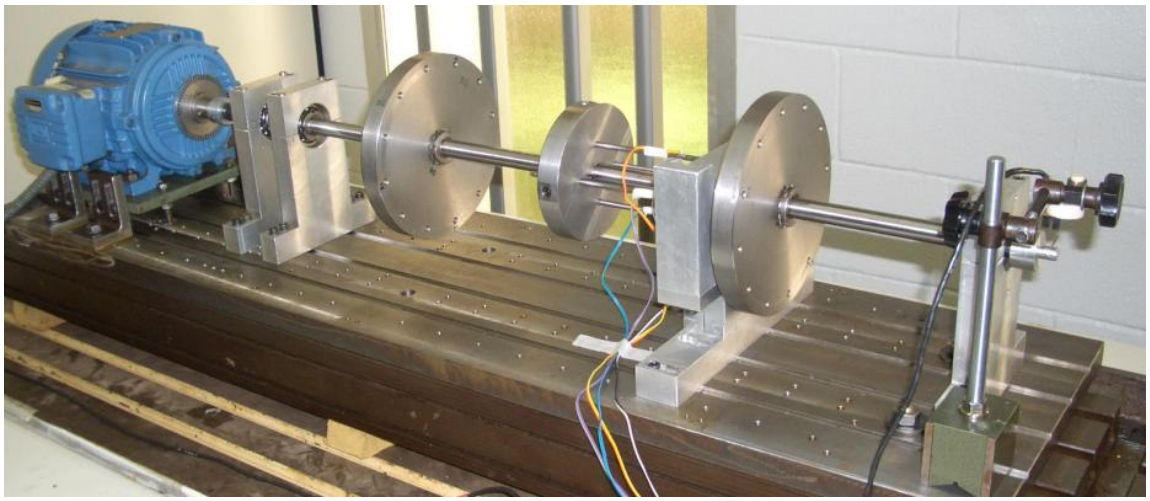

Figure 3. Experimental arrangement of the rotor system.

In order to simulate better the real process of the rub-impact, a device was designed for making possible a full rub experiment. It is easy to change the material that suffers the rubbing forces and the friction coefficient can be changed too. Also in Fig. 4 is shown the facility of changing the stiffness of this device by changing its location along the bars.

There is one uniaxial strain gage in each bar in longitudinal direction to measure the quantity of rub force applied during the experimental tests. Each bar has 5 mm of diameter and each strain gage has base size of 4.8 x 2.4 mm and gage length of 1mm.

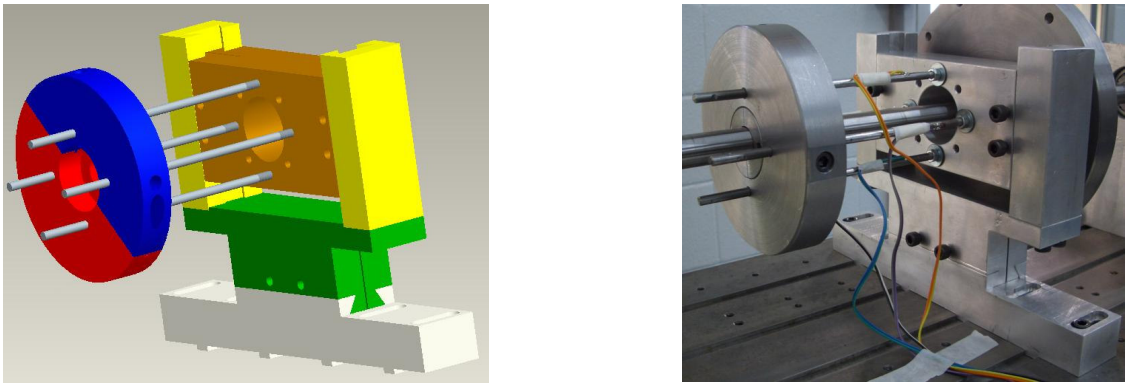

Figure 4. Measurement device of the rubbing forces. (a) Design. (b) Real.

The impact stiffness coefficient of the seal k_R was set according to the physical limit of the test rig. The biggest value of k_R is related to as near as the mass can stay from the strain gage, and the other hand, the smallest value of k_R is related to as far as the mass can stay to reach the point of measurement avoiding that the device's base touch one of the disks.

The eddy current transducers are used to measure the displacement of the shaft at some possible positions which is linked to the finite elements model, and at these specified positions, the test rig is able to measure in vertical and horizontal direction. The shaft acceleration was monitored by one tachometer which emits 5 volts each time one mark in the shaft pass through this sensor.

The experimental data acquired from the eddy current transducers, strain gages and tachometer are amplified according to their necessities, received by the data-acquisition card and finally sent to the computer for recording. The data acquisition card can receive 16 channels of signal simultaneously and its sampling frequency can reach a maximum of 1250 kHz.

5. RESULTS

Both simulated and experimental results were accomplished with the objective of detecting the dynamic behavior of the effects produced by the rubbing between the shaft and mechanical seal.

The time and position which rub occurs cannot be predicted. During the start and finish periods of the partial rub, sudden appearance and disappearance of the contact will cause a rapid change in the system momentum and therefore leads to an impact on the system. This corresponds to the introduction of a wideband excitation to the system and the complicated transient responses are thus caused in the system (Chu and Lu, 2005). During the process, the friction will result in wear and thermal effect which will change the coefficient of friction and increase the unbalance. In the order to avoid secondary malfunctions due to the rubbing by keeping the frequencies in dangerous ones, in all of the results the transient response was simulated numerically, and also the experimental test was done in such way that the system accelerates from the rest up to 400 rad/s in 20 seconds ($\alpha = 20$ rad/s^2) guaranteeing the non-stationary behaviour of the system.

The finite element rotor model in Fig. 2 shows the simulated model about a rotor system with 2 disks on the shaft supported by 3 bearings totalizing 14 elements and 10 nodes. The unbalance is $U = 1 \times 10^{-4}$ m. The static clearance δ between the shaft and seal is fixed a parameter in all of the simulated cases and its value is equals to 0.5 mm. The variable parameters are described in the Tab. 1.

Some researches have accomplished experimental tests in order to obtain the value of friction coefficient for using in their works. In special, Bartha (2000) could obtain values of the coefficient of lubricated friction (f approximately equals to 0.2) and dry friction (f varying between 0.2 and 0.6).

Table 1. Parameters for each test.

Test Number	Figure Concerned	k_R [N/m]	f	Contact Surface
1 (simulated)	Fig. 5	1.3×10^5	0.6	-
2 (simulated)	Fig. 6	4.48×10^4	0.2	-
3 (experimental)	Fig. 7	1.3×10^5	-	rough
4 (experimental)	Fig. 8	4.48×10^4	-	lubricated and polished

Accelerating from the rest up to 400 rad/s, the complete process of rub happens since slight to serious rub. It starts when the shaft touches by the first time on the seal until the end of contact when the vibration amplitudes of the rotor centers itself in frequencies higher than the first natural one which is around 220 rad/s.

From the Fig. 5 up to 8, in the right side are being illustrated the radial motion of the shaft, vertical component of motion on top left, and vertical component of rub force on bottom left. For these four figures, the value of static clearance between the outer shaft surface and inner seal one was set as 0.5 mm.

During the run-up, just after the contact gets starts, first forward whirl occurs and suddenly the motion turns to backward whirl with larges deflections (Ehehalt and Markert, 2002). For the simulations 1 and 2, is easily noted that when the deflection reaches the static clearance in 0.5 mm, the rotor dynamic behaviour has changed by the rub forces illustrated in black line. And also, the contact finishes with the shaft returning to smaller self centered deflections around 270 rad/s in 13.5 seconds when the forces are annulled for the Fig. 5 and around 240 rad/s in 12 seconds for the Fig 6.

The unstable behavior appears clearly between 230 and 270 rad/s for the case which the stiffness and the coefficient of friction were bigger in the test 1. In the other hand, this feature is missing in the test 2 which these values are smaller. The features are similar for the experimental tests 3 and 4, but as the simulation does, for bigger stiffness, bigger rub forces happens too.

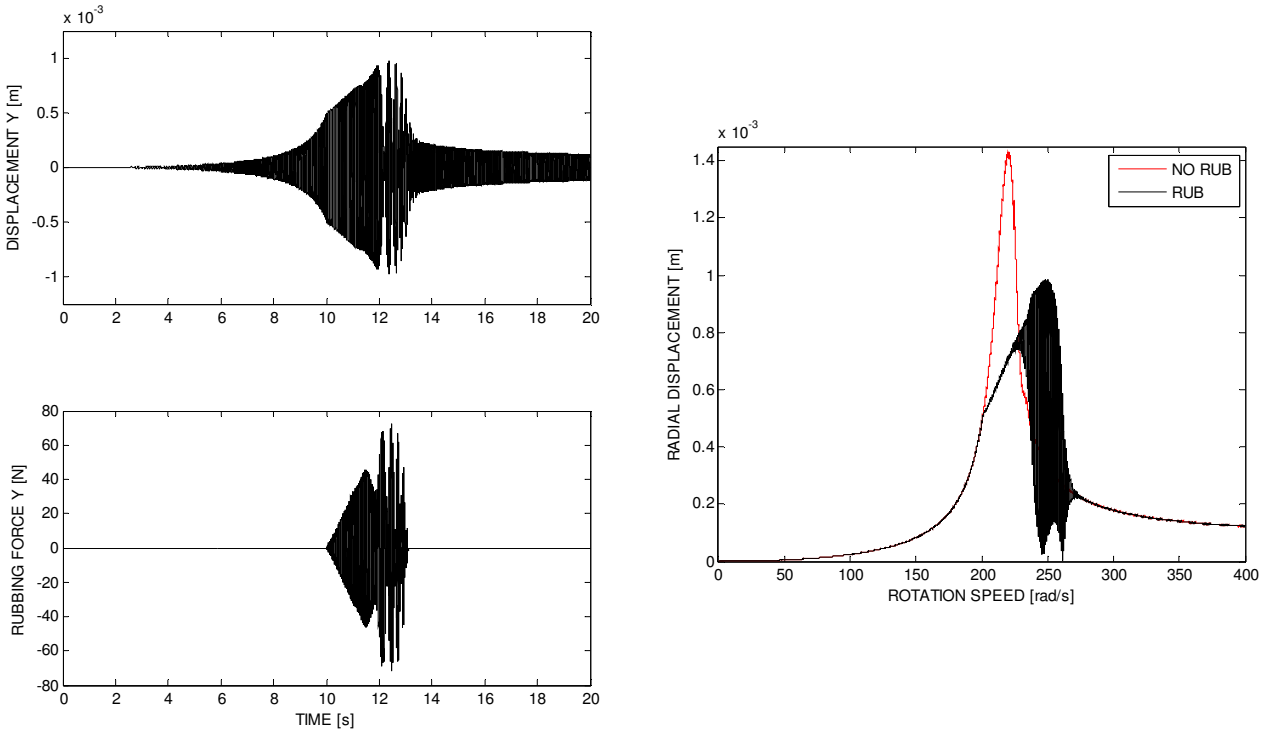

Figure 5. Simulated radial motion of the shaft at seal position or node 9 (right), vertical component of motion (top left) and vertical component of rub force at the node 6 (bottom left).

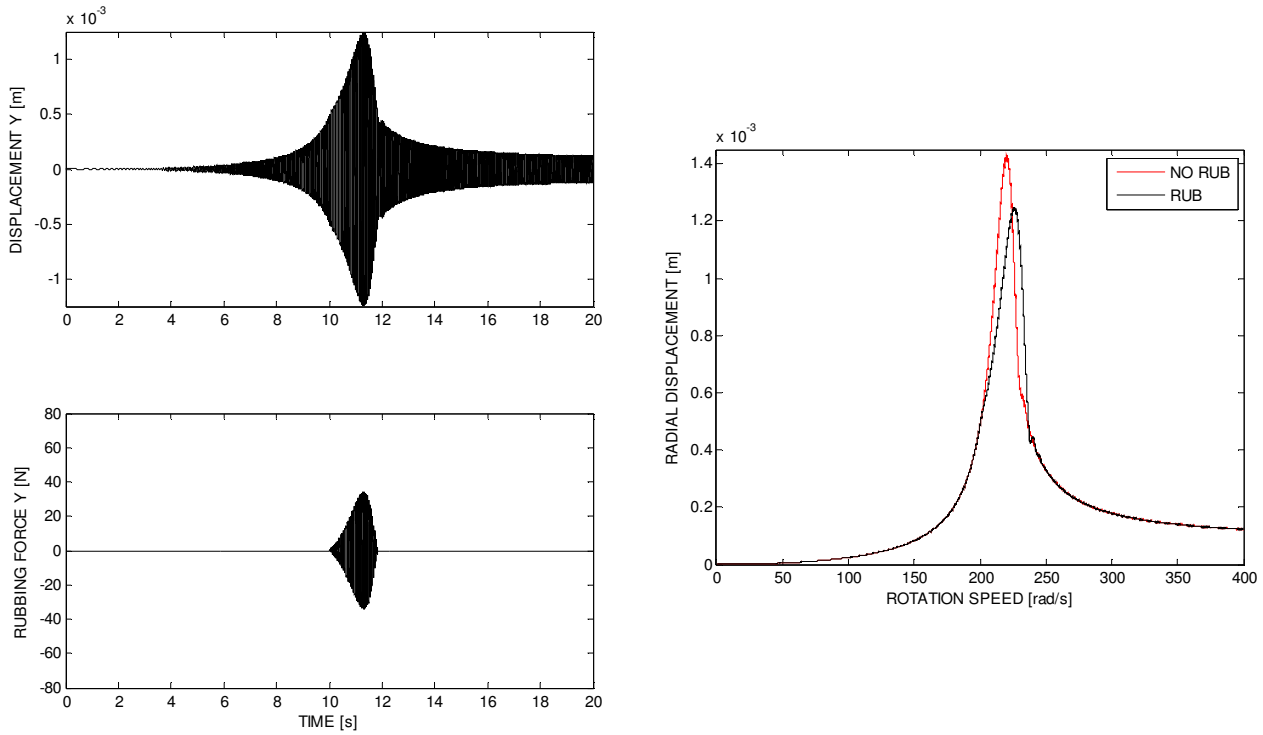

Figure 6. Simulated radial motion of the shaft at seal position or node 9 (right), vertical component of motion (top left) and vertical component of rub force at the node 6 (bottom left).

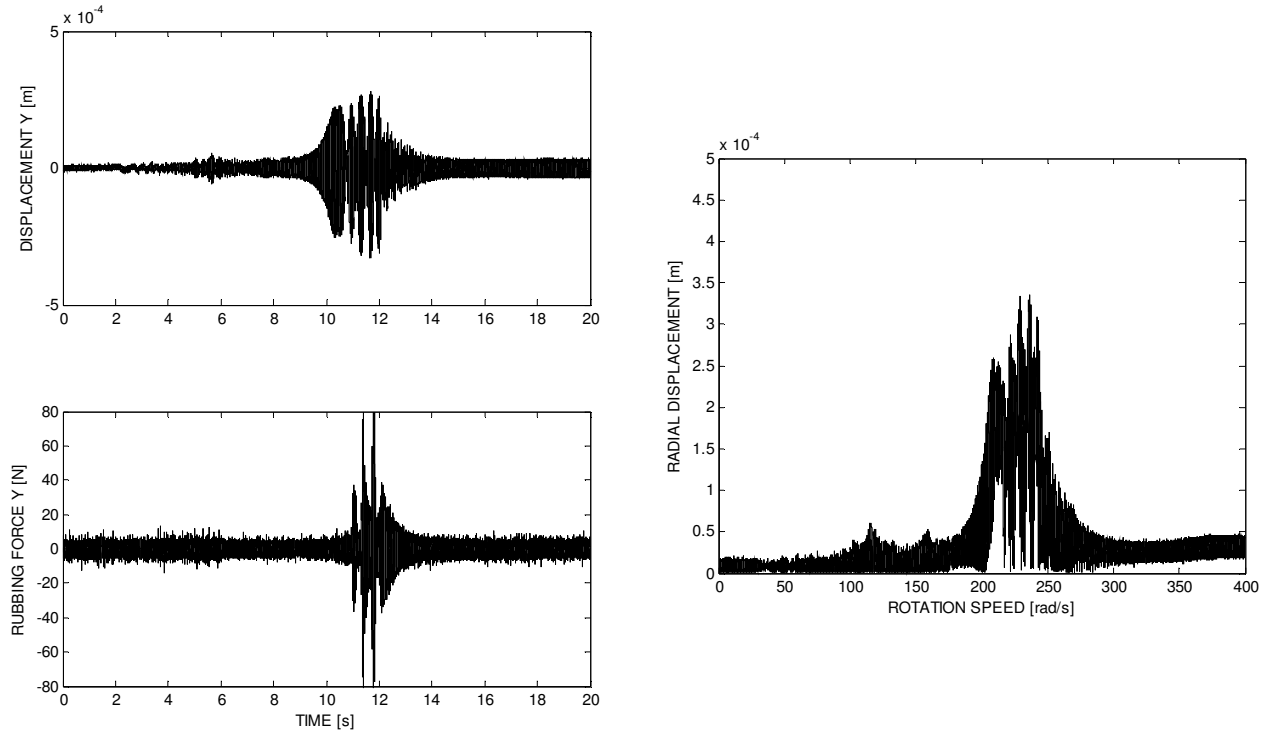

Figure 7. Experimental radial motion of the shaft measured at the node 9 (right), vertical component of motion (top left) and vertical component of rub force at the node 6 (bottom left).

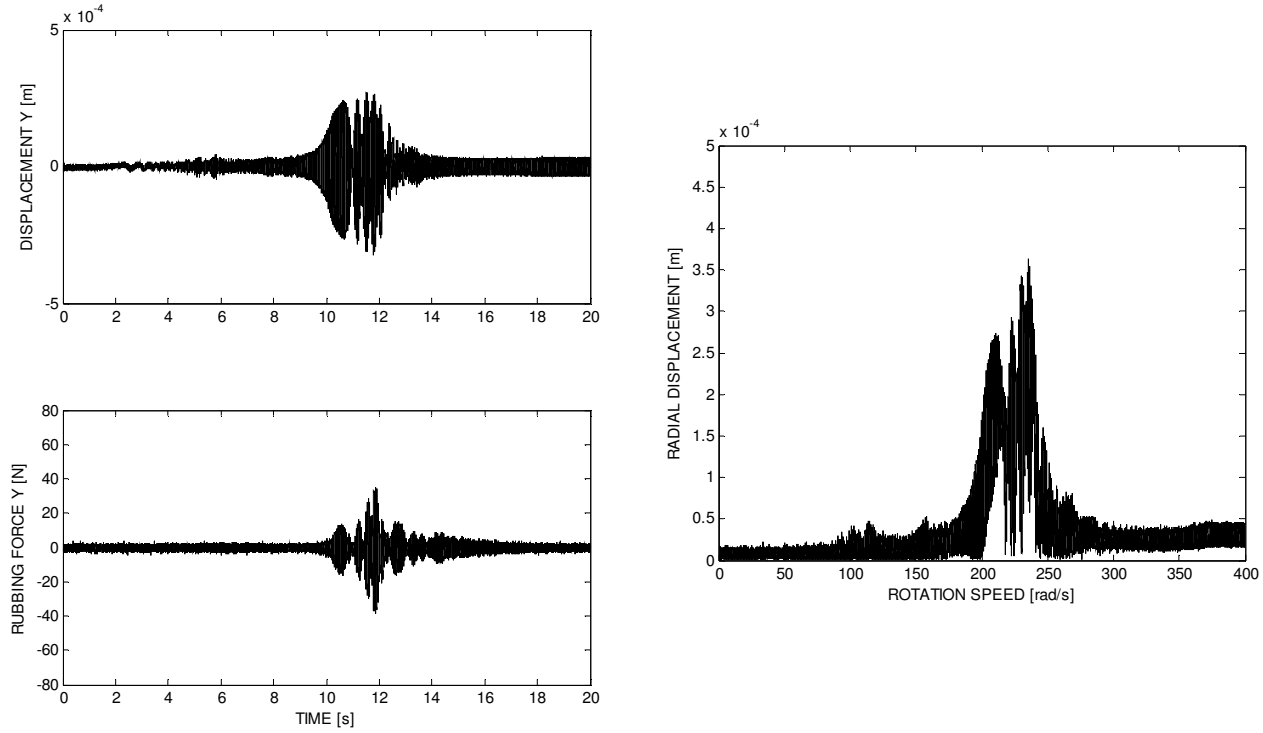

Figure 8. Experimental radial motion of the shaft measured at the node 9 (right), vertical component of motion (top left) and vertical component of rub force at the node 6 (bottom left).

6. DISCUSSIONS AND CONCLUSION

The test rig was able to measure the rubbing forces of the multi rotor system for transient response as well as the finite element model for the same system did.

Theoretically, the rubbing forces before and after the impact period should be null as the simulated tests show before 10 seconds and also after 13.5 and 12 seconds in the Fig 5 and 6 respectively. But in the experimental tests 3 and 4 were observed non-null values, perhaps it is due to the position where the strain gages were positioned being excited by the foundation.

The excessive vibration around 120 and 160 rad/s in the experimental tests number 3 and 4 might be a result of higher frequencies being excited by the misalignment effects.

For experimental tests, the large deflections through the first natural frequency of the system were impeding the location of the sensors at that position, and for this reason, these eddy current sensors were located at the node number 9, although the rubbing device was kept at the node number 6. Thus, the simulations were done for showing both deflections and rub forces at same position where the experiments were did, nodes 9 and 6 respectively.

The eddy current sensors are able to be located at the nodes 3, 5, 6, 7 and 9 on the experimental test rig. Nevertheless, the number of nodes of the system was did not only about to represent these positions but also for ensuring that analysed frequencies must be under the maximum natural frequency of the model, which is around 7000 Hz.

The strain gage size was designed for ensuring that orthogonal deflections in relation to the plane of measurement could be negligible, that was verified during the sensor calibration. The time during the occurrence of the rubbing is very short, consequently, the thermal effects were judged suitable to be neglected, but the inertia effects of sensor mass in Figure 4 should be not neglected. However, the results show that natural frequencies of the sensor are insignificants or even they are far from the analyzed range of frequencies, otherwise, it should appear into the experimental rubbing forces. Anyway, the insertion of the missing effects is hoped to be done for becoming the dynamical model more realistic and distinguish the rub features by wavelets analysis.

7. ACKNOWLEDGEMENTS

The authors would like to acknowledge CNPq (National Counsel of Technological and Scientific Development) for supporting this work.

8. REFERENCES

Aquino, M.B., Nordmann, R. and Pederiva, R., 2006, “Transient response simulation of shaft/seal rubs in a rotor supported by non-linear hydrodynamic forces”, 7th IFToMM - Conference on Rotor dynamics, Vienna, Austria, Paper ID 255.

Bedoor, B.O.Al-, 2000, “Transient torsional and lateral vibrations of unbalanced rotors with rotor-to-stator rubbing”, Journal of Sound and Vibration, v 229(3), pp 627-645.

Bartha, A.R., 2000, “Dry friction backward whirl of rotors”. Ph.D. Dissertation, Swiss Federal Institute of Technology Zurich, 212p.

Bently, D.E., Yu, J.J., Goldman, P. and Muszynska, A., 2002a, “Full annular rub in Mechanical Seals, Part I: Experimental results”. International Journal of Rotating Machinery, v 8(5), pp 319-328.

Bently, D.E., Goldman, P. and Yu, J.J., 2002b, “Full annular rub in Mechanical Seals, Part II: Analytical study”. International Journal of Rotating Machinery, v 8(5), pp 329-336.

Chu, F. and Lu, W., 2001, “Determination of the rubbing location in a multi-disk rotor system by means of dynamic stiffness identification”. Journal of Sound and Vibration, v 248(2), pp 235-246.

Chu, F. and Lu, W., 2005, “Experimental observation of nonlinear vibrations in a rub-impact rotor system”. Journal of Sound and Vibration, v 283, pp 621-643.

Ehehalt, U., Hahn, E. and Markert, R., 2005, “Motion patterns at rotor stator contact”. Proceedings of IDETC/CIE, ASME, Long Beach, California, USA, 13 p.

Ehehalt, U. and Markert, R., 2002, “Rotor motion during stator contact”, Proceedings IFToMM, Sydney, Australia,v II, pp 913-920.

Ehehalt, U., Hochlenert, D, Markert, R. and Weber, H.I., 2006a, “Approximate description of backward whirl at rotor-stator-contact”, Advances in vibration control and diagnostics, Polimetrica International Scientific Publisher, Monza, Italy, pp 65-82.

Ehehalt, U., Markert, R. and Hahn, 2006b, “Rotor stator contact – Measured Motion Patterns”, Advances in vibration control and diagnostics, Polimetrica International Scientific Publisher, Monza, Italy, pp 83-98.

Ehehalt, U., Markert, R. and Wegener, G., 2006c, "Synchronous forward whirl at rotor-stator-contact – stability investigation", Advances in vibration control and diagnostics, Polimetrica International Scientific Publisher, Monza, Italy, pp 99-113.

Fatarella, F. 1999, "On the dynamics of reverse whirl due to rotor/stator interaction". Ph.D. Dissertation, Imperial College of Science, Tecnology & Medicine, London, 195p.

Lalanne, M. and Ferraris, G., 1999, "Rotordynamics prediction in engineering", John Wiley and Sons, 2nd ed., Chichester, 254p.

Muszynska, A. and Goldman, P., 1995, "Chaotic responses of unbalanced rotor/bearing/stator systems with looseness or rubs". Chaos, Solitons & Fractals, v 5, pp 1683-1704.

Piccoli, H.C., 1994, "Chaos observation in measurements of a rotor motion submitted to rubbing". (In Portuguese), Ph.D. Dissertation, UNICAMP, Campinas, 144p.

Sawicki, J.T., Bravo, A.M. and Gosiewski, Z., 2003, "Thermomechanical behavior of rotor with rubbing". International Journal of Rotating Machinery, v 9(1), pp 41-47.

Schettel, J. and Nordmann, R., 2004, "Modeling flow induced forces in turbine labyrinth seals". Flow induced Vibration, de Langre & Axisa ed, École Polytechnique, Paris, 6-9th July.

Wegener, G. and Markert, R., 1998, "Influence of contact and impacts on the dynamics of na elastic rotor with an elastic retainer bearing". V.I. Babitsky (Ed.): Dynamics of Vibro-Impact Systems - Proceedings of the EUROMECH Colloquium.

Wegener, G., Markert, R. and Pothmann, K., 1998, "Steady-state-analysis of a multi-disk or continuous rotor with one retainer bearing". Proceedings, Fifth International Conference on Rotor Dynamics, IFToMM, pp 816-828.

Zhang, Y.M., Wen, B.C. and Liu, Q.L., 2003, Reliability sensitivity for rotor-stator systems with rubbing. Journal of Sound and Vibration, v 259(5), pp 1095-1107.

9. RESPONSIBILITY NOTICE

The authors are the only responsible for the printed material included in this paper.